

數學建模 科學研究 颱風動力

郭鴻基
教育部國家講座教授
臺大終身職特聘教授

Politics are for the moment
An equation is for eternity

9/22/2009
臺大大氣科學系

Now we only see models,
like reflections in a mirror;
but then we shall see face to face.
Now I only know partially;
but then I shall know as fully as
I am myself known.

St. Paul, 1st letter to the Corinthians, 13:12

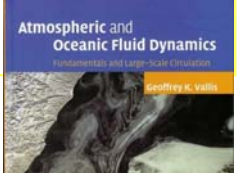
Models、經典、聖哲就如鏡子，讓我們看到自己，讓我們瞭解自己的侷限，更進而體會完整的人性。

「數學科學模式」幫助我們由片面觀察的自然界，統會瞭解共通完整的科學定律。

2

20th Century

Geophysical Fluid Dynamics (GFD)
Atmospheric Oceanic Fluid Dynamics (AOFD)
is for those interested in doing research in the physics, chemistry, and/or biology of Earth fluid environment.

(a) 
(b) 

Atmospheric and Oceanic Fluid Dynamics
Fundamentals and Large-Scale Circulation
Geoffrey K. Vallis

Fig. 9.2 Karman vortex streets in (a) the laboratory, for water flowing past a cylinder [From M. Van Dyke, *An Album of Fluid Motion*, Parabolic Press, Stanford, Calif. (1982) p. 56.], and (b) in the atmosphere, for a cumulus-topped boundary layer flowing past an island [NASA MODIS imagery].

熱力學 + 流體力學

Euler 1755 $\frac{d}{dt} \int_{v_m} \rho \vec{v} dv = - \int_{\partial v_m} p d\vec{s}$

$\int_{v_m} \rho \frac{d\vec{v}}{dt} dv = - \int_{v_m} \nabla p dv$

Lagrange 1781 $\frac{d\vec{v}}{dt} = -\nabla p$
Rotation , Vortex

Lorentz Force Law $\mathbf{F} = q(\mathbf{E} + \mathbf{v} \times \mathbf{B})$
 $\mathbf{F} = q(-\nabla V + \mathbf{v} \times \mathbf{B})$

Helmholtz 1858 $\frac{\partial \vec{\zeta}}{\partial t} + \vec{v} \cdot \nabla \vec{\zeta} + \vec{\zeta} \cdot \nabla \cdot \vec{v} = \vec{\zeta} \cdot \nabla \vec{v} + \vec{B}$
 $\vec{B} = \nabla \times (-\frac{1}{\rho} \nabla p)$

19世紀煙圈表演 

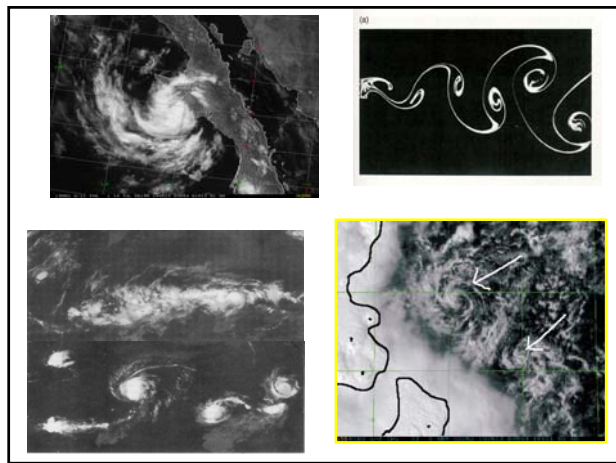
Wake Turbulence

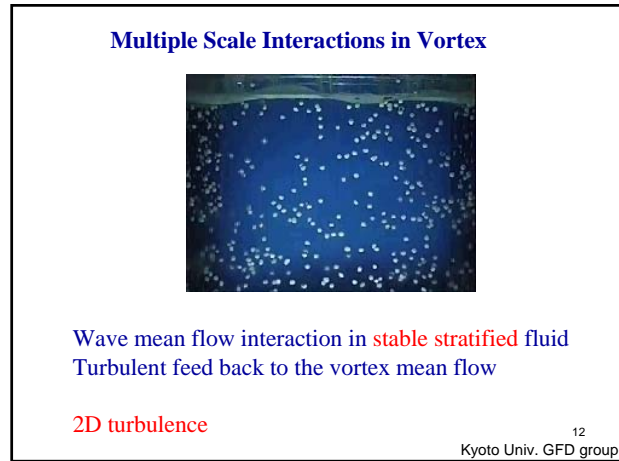
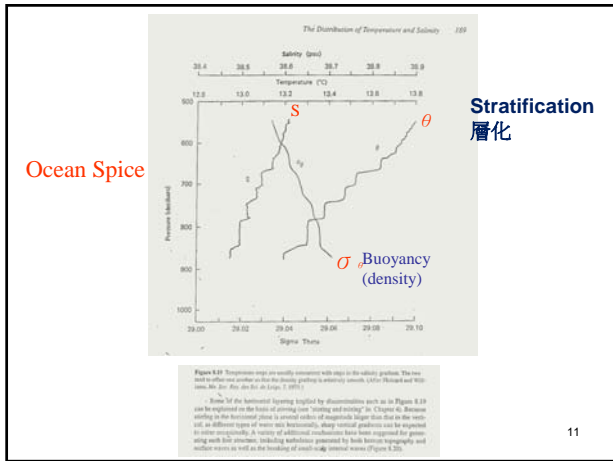
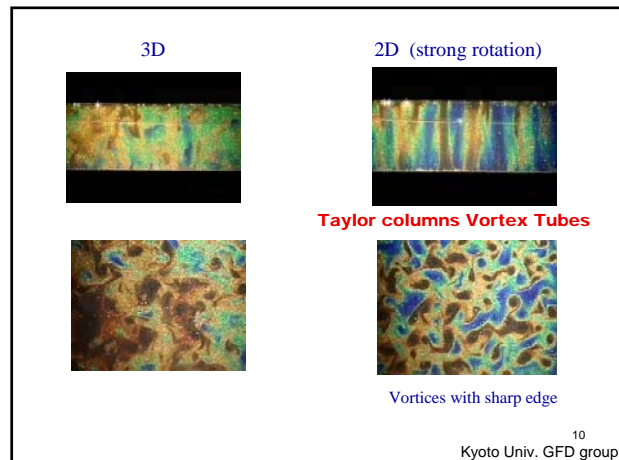
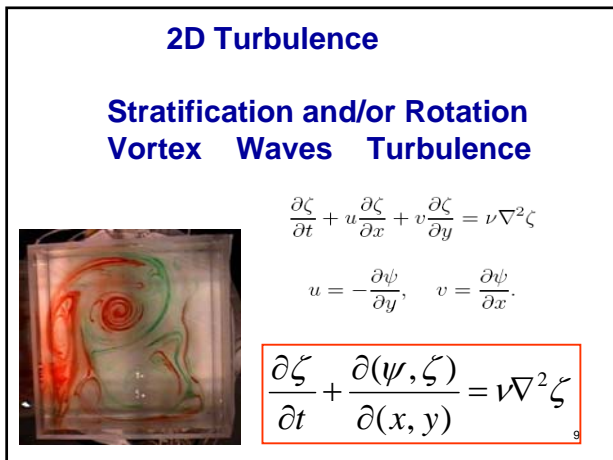
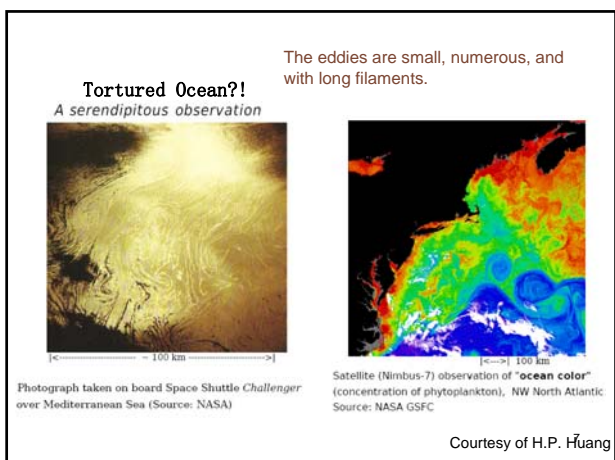
Fig. 8.10. Sketch of the flow along an airfoil. The wing is shown in contour C is shown by the thick solid line.

Fig. 8.10.3 (a) A series of olive vortex representing a wing with a uniform lift distribution. (b) Lift distributions on an off-the-wing.

Fig. 8.10.4 The vortices in the wake of an oncoming wing, idealized under the hypothesis that the lift fluctuation is very small so that the distortion of the wake due to the vortices in it is also very small. L is the lift, α is the angle of attack.

Fig. 8.10.5 The vortex wake behind a stork in level flight.





Non-divergent barotropic model (Nearly Inviscid Fluid)

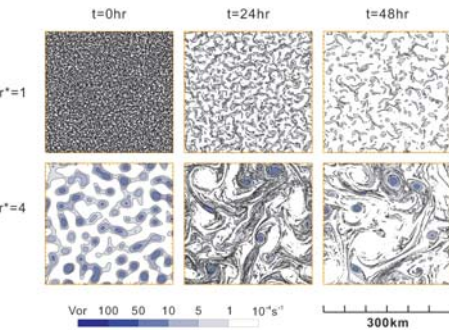
$$\frac{\partial}{\partial t} \zeta + J(\psi, \zeta) = v \nabla^2 \zeta \quad \boxed{\nabla^2 \psi = \zeta}$$

The energy and enstrophy relations

$$\begin{aligned} \frac{dE}{dt} &= -2v\zeta & E = \iint \frac{1}{2}(u^2 + v^2) dx dy & \text{kinetic energy} \\ \frac{d\zeta}{dt} &= -2v\varphi & \zeta = \iint \frac{1}{2}\zeta^2 dx dy & \text{enstrophy} \\ \frac{d\varphi}{dt} &= -2v\zeta & \varphi = \iint \frac{1}{2}\nabla\zeta \cdot \nabla\zeta dx dy & \text{palinstrophy} \end{aligned}$$

Batchelor 1969

13



Fewer and stronger vortices !!!
Coherent structure with filamentations
in 2-D turbulence

14

Weiss(1981,1991), Rozoff et al. (2004)

$$\begin{aligned} \frac{D}{Dt}(\nabla\zeta) &= -J(\nabla\psi, \zeta) \\ \rightarrow \nabla\zeta(t) &\propto \exp(\lambda t) \quad \lambda = \pm \frac{1}{2}\sqrt{Q} = \pm \frac{1}{2}\sqrt{S_1^2 + S_2^2 - \zeta^2} \\ S_1 &= \frac{\partial u}{\partial x} - \frac{\partial v}{\partial y} \quad (\text{stretch deformation}) \\ S_2 &= \frac{\partial v}{\partial x} + \frac{\partial u}{\partial y} \quad (\text{shear deformation}) \end{aligned}$$

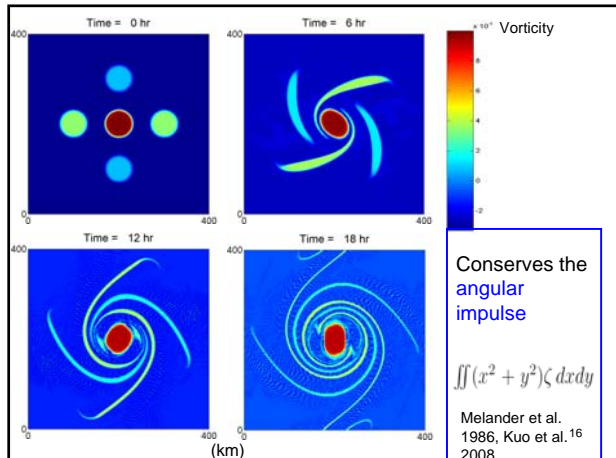
$Q > 0$ (strain dominates)

→ vorticity gradient will be stretched

$Q < 0$ (vorticity dominates)

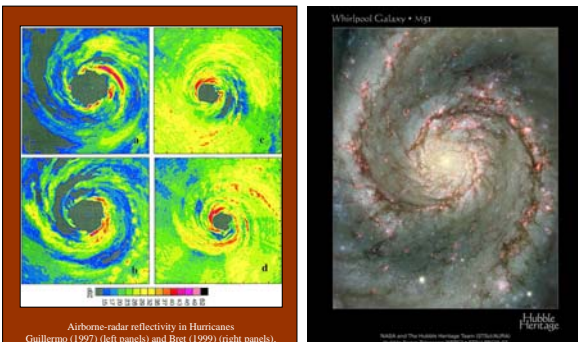
→ vortex is stable (survival of eyewall meso-vortices)

15



Conserves the angular impulse
 $\iint(x^2 + y^2)\zeta dx dy$
Melander et al.
1986, Kuo et al.
2008

Spiral Band in Hurricane and Galaxy



Kossin and Schubert 2001

17

Electron density redistribution in experimental plasma physics

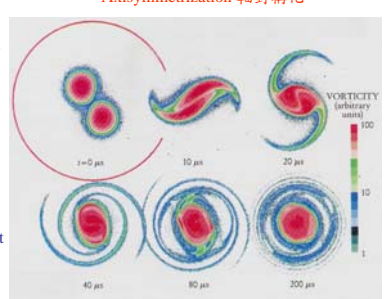
single sign charge
+
axial magnetic field confinement

$$\mathbf{E} = -\nabla\psi$$

$$\nabla \cdot \mathbf{E} = -\nabla^2\psi = \frac{\rho}{\epsilon}$$

\mathbf{B}
 \mathbf{E}
 $\bar{\mathbf{E}} \times \bar{\mathbf{B}}$
drift

Coriolis force



Core is protected, thin filaments from edges

18

Bowman and Mangus (1993)

臭氧洞衛星觀測

Observations of deformation and mixing of the total ozone field in the Antarctic polar vortex

核心空氣被渦旋鎖住

細絲帶

Fig.1: Daily TOMS images of total ozone in the Southern Hemisphere for six consecutive days in October 1983. Latitude circles are drawn at 40°, 60°, and 80° S. The outermost latitude is 20° S.

19

Huang and Robinson 1998

Forcing added

Inverse energy cascade to zonal Harmonics

$P_n^m(\mu)$

Spherical Harmonics

Fig. 2. Energy spectrum $E(m, n)$ of an ensemble mean at day 80 of 10 decaying turbulence experiments. The magnitude of the spectrum is normalized by the maximum value on the map. Contour levels are 0.0001, 0.001, 0.01, 0.1–0.9 with increment 0.1. Area with $E(m, n) > 0.1$ is lightly shaded, $E(m, n) > 0.2$ heavily shaded.

Jupiter Rotational period 9.84hr

Huang and Robinson 1998

The Great Red Spot

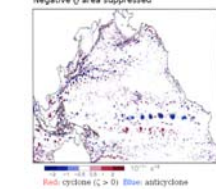
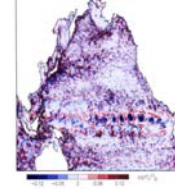
Fig. 4. Time-averaged zonal-mean zonal wind profiles for case I-VII in Table 1 (the eight open circles in Fig. 3). Black grid on the abscissa represents 1 m s⁻¹.

Fig. 4. Time-averaged zonal-mean zonal wind profiles for case I-VII in Table 1 (the eight open circles in Fig. 3). Black grid on the abscissa represents 1 m s⁻¹.

Vorticity at surface (snapshot)

Map of $\zeta \text{ and } \zeta \theta$ (snapshot)

Negative ζ area suppressed



Show is ζf (ζ = Rossby number, Ro), f = Coriolis parameter at 35°N

$Ro = \zeta / (0.1)$ in midlatitude over the North Pacific

$\zeta < 0$ (Red) cyclone ($\zeta > 0$) (Blue) anticyclone

Vertical extent of the vortices

Isentropic vorticity parameter $Q = 4.7 \times 10^{-4}$

Index of Kolmogorov parameter index

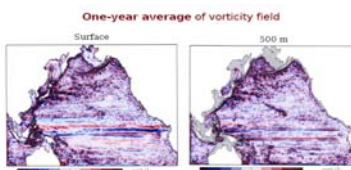
Box 1

Box 2, axis (shown only) w/ boxes are similar

Courtesy of H.P. Huang

Mid-latitude eddies are deeper

Satellite observations



Multiple zonal-jet like structures emerge with long-term average

- The presence of multiple zonal jets can critically affect the transport of heat, biota, and chemical constituents that are important for climate and life on Earth.

Eddy diffusivities for tracer transport along and across zonal jets are dramatically different (e.g., Smith 2005)

- Clarification of the interaction between eddies/zonal jets and ocean gyre may lead to revision of the conventional view of ocean gyre.

Courtesy of H.P. Huang

一杯咖啡，古今往事盡付笑談中。

The best part of waking up, is the vortex in your cup!

$$\frac{D\theta}{Dt} = \frac{\partial \theta}{\partial t} + \vec{V} \cdot \nabla \theta = v \nabla^2 \theta$$

$$C = \frac{1}{2} \int \nabla \theta \cdot \nabla \theta dV$$

$$\frac{dC}{dt} = \int (\vec{V} \cdot \nabla \theta) \nabla^2 \theta dV - v \int (\nabla^2 \theta) dV$$

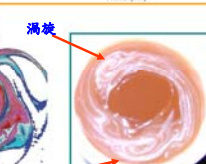
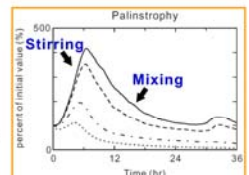
Stirring Mixing

Coffee with white

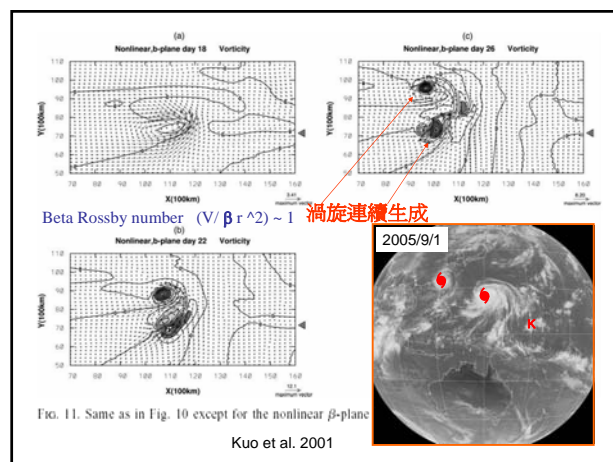
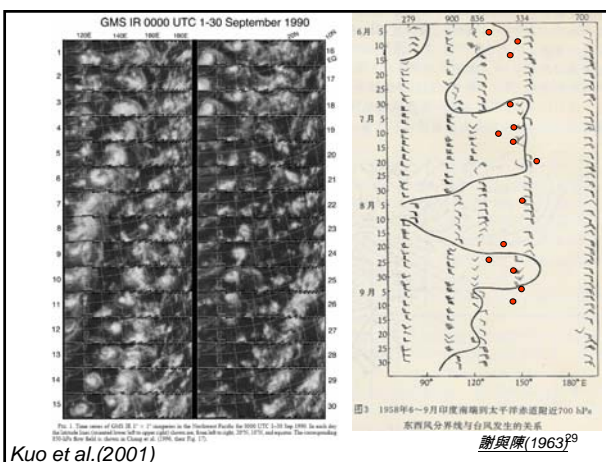
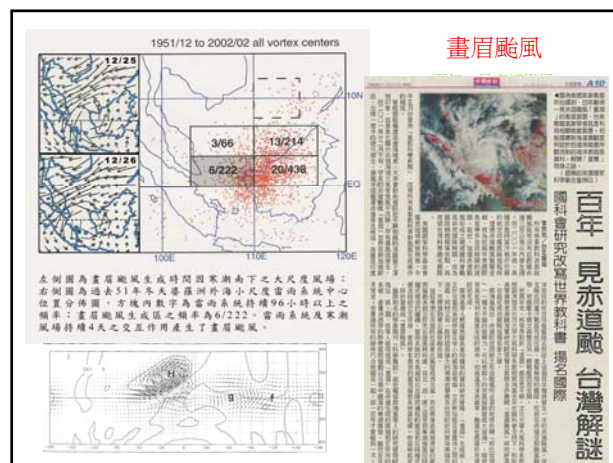
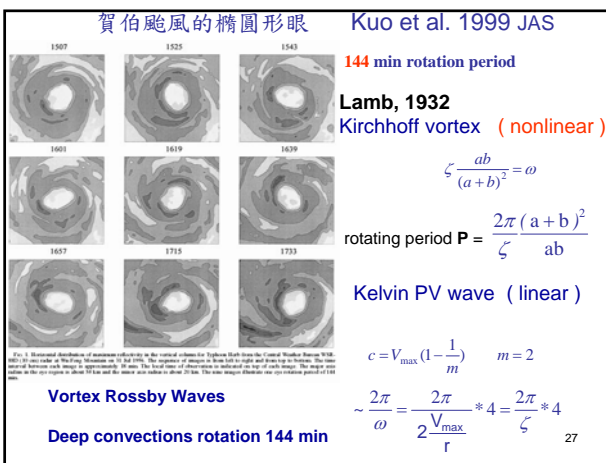
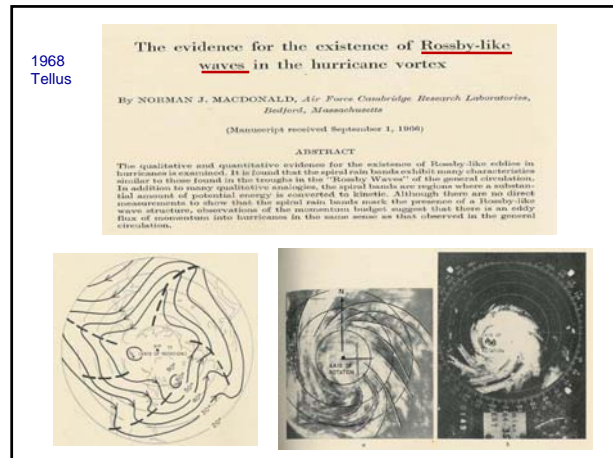
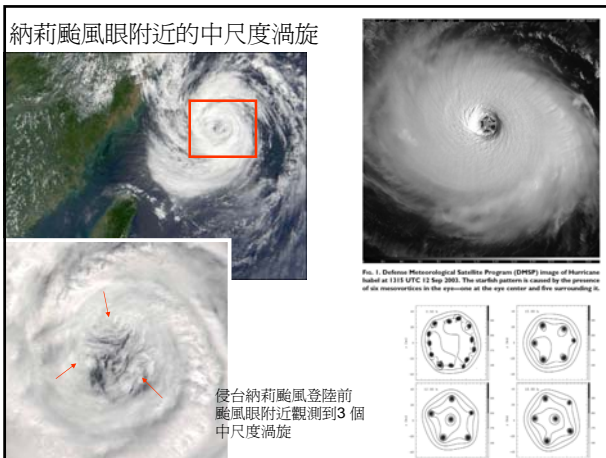
12 hr

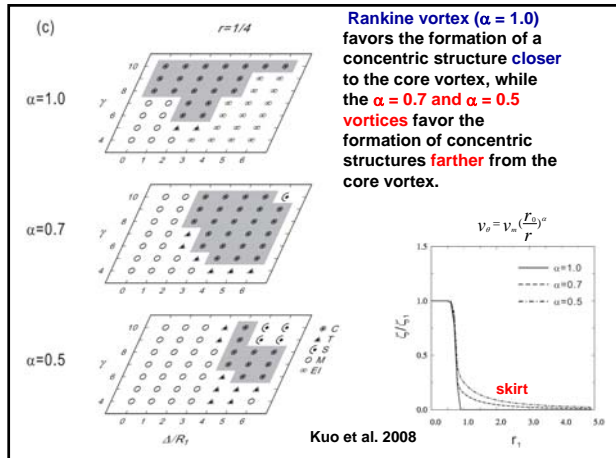
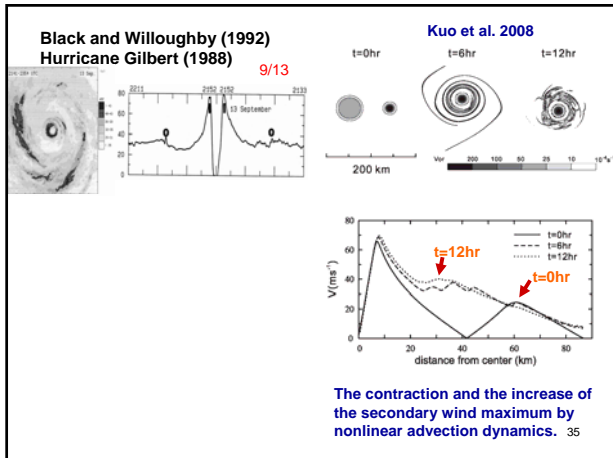
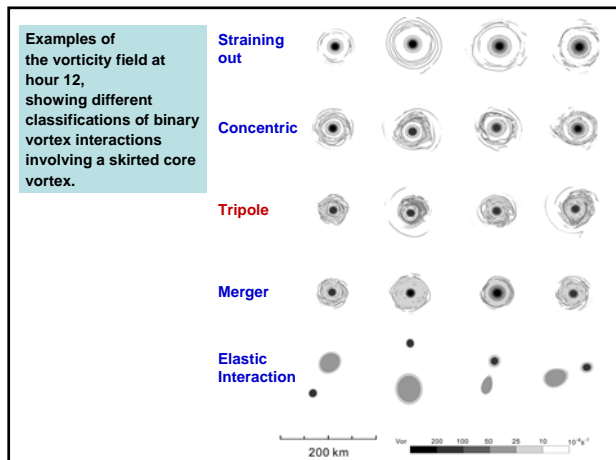
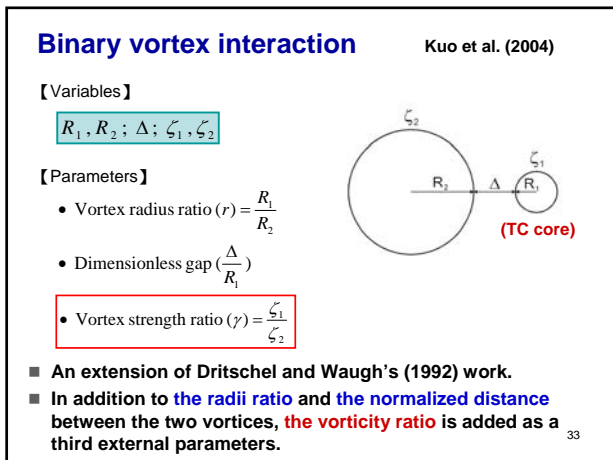
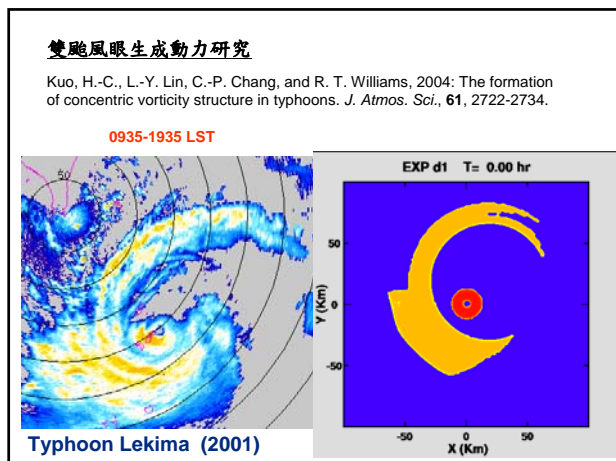
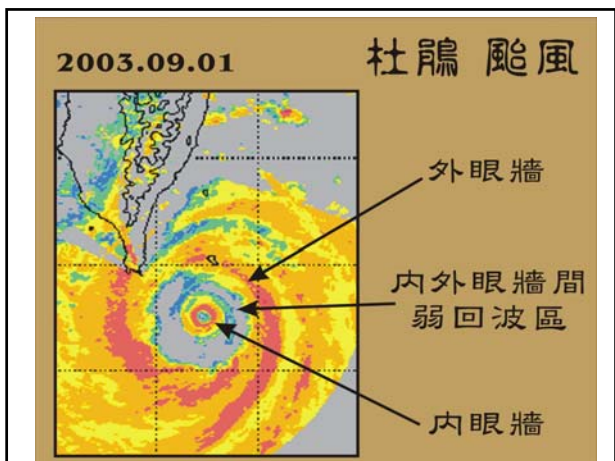
Stirring

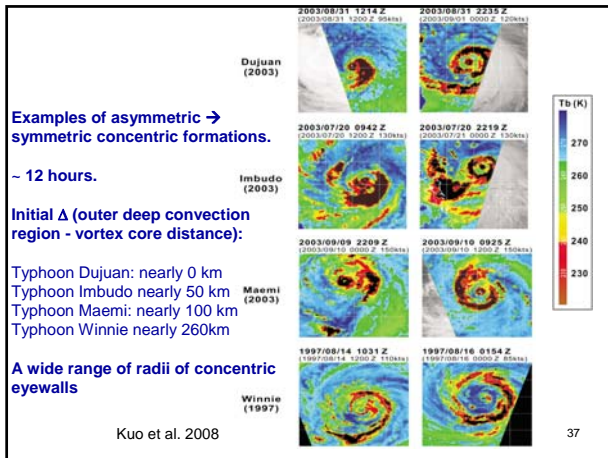
Mixing



4







Terwey and Montgomery, June JGR 2008

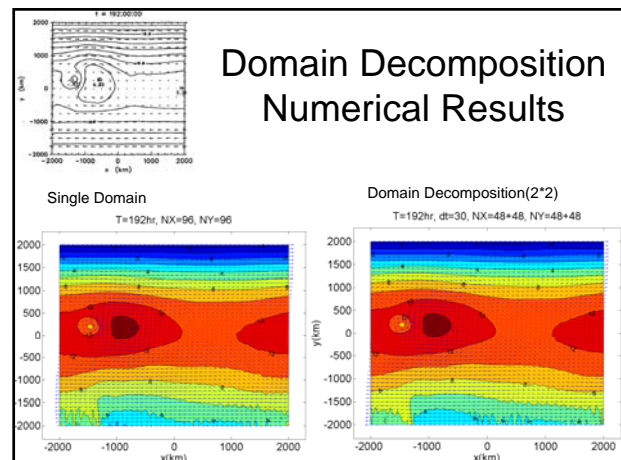
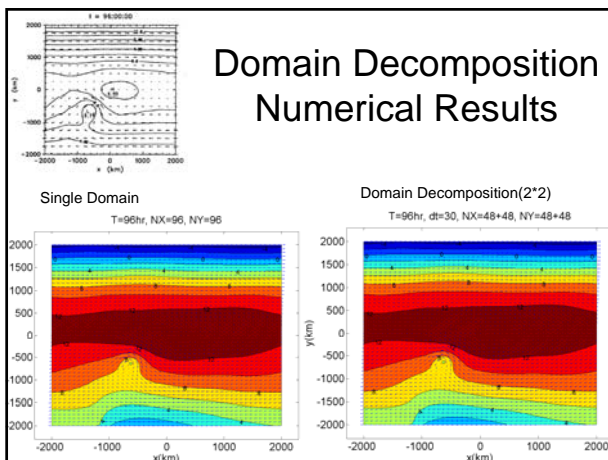
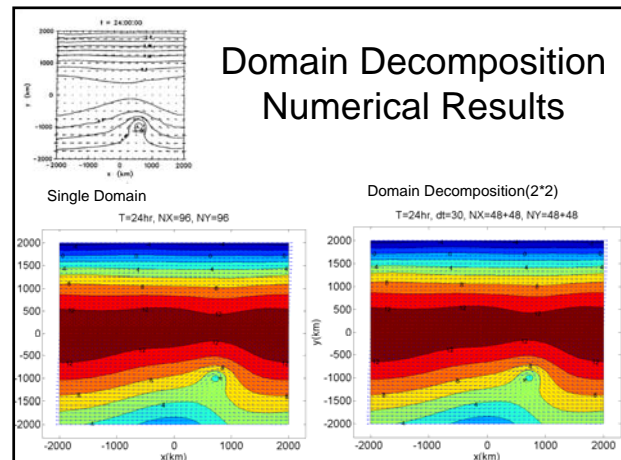
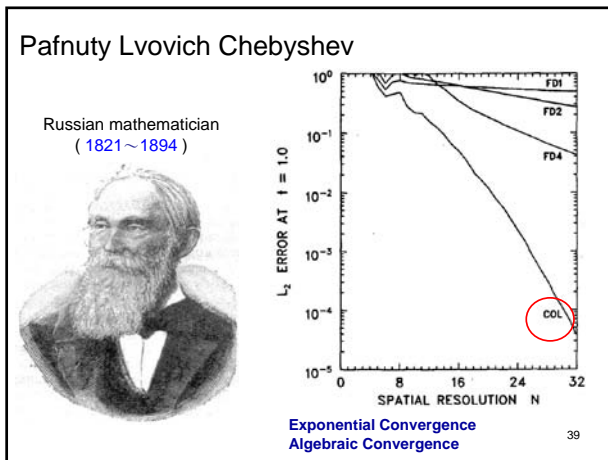
D12112 TERWEY AND MONTGOMERY: MODELED SECONDARY EYEWALL FORMATION D12112

Table 1. List of Secondary Eyewall Formation Hypotheses With Summary of Relevance to our Model Hurricanes^a

Authors	Hypothesis Summary	Reference to Current Model Results	Type
Hilloughby et al. [1982]	Downdrafts from the primary eyewall force a ring of convection to form.	Few downdraft-forced updrafts during this time	O
Homann from the squall line research of Zinger [1977]	Interference between local inertia period and asymmetric friction due to storm motion.	No systematic storm motion in the simulated storms.	A
Hilloughby [1989]	Topographic effects	No topographic forcing in the simulations.	O
Hawkins [1983]	Ice microphysics	"Watts-rain" (no-ice) sensitivity case also produces secondary eyewall.	A
Hilloughby et al. [1984]	Synoptic-scale forcings (e.g., inflow surges, upper-level momentum fluxes)	No synoptic scale forcings in the simulations	O
Molinari and Shabot [1985] and Molinari and Villaro [1989]	Internal dynamics-asymmetrization via wave breaking, shear-wave processes, collection of wave energy near stagnation or convergence zones.	Possible explanation	N
Montgomery and Kallenbach [1997], Camp and Montgomery [2001] and Terwey and Montgomery [2001]	Stagnated eddy momentum fluxes and WISHL feedback	Possible explanation	A
Norris and Gutzler [2003]	Asymmetrization of positive vorticity perturbations around a strong and tight core	Possible explanation	N
Kuo et al. [2004, 2008]			

^aThe type column refers to the type of model or observations that were used to formulate the hypothesis. O stands for observationally-based; A stands for axisymmetric model; N stands for nonaxisymmetric model.

38

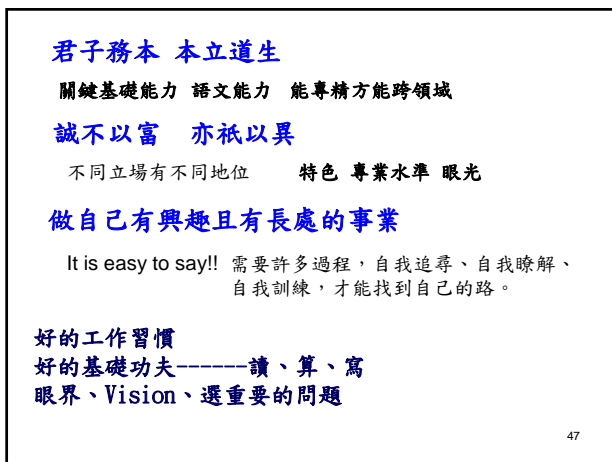
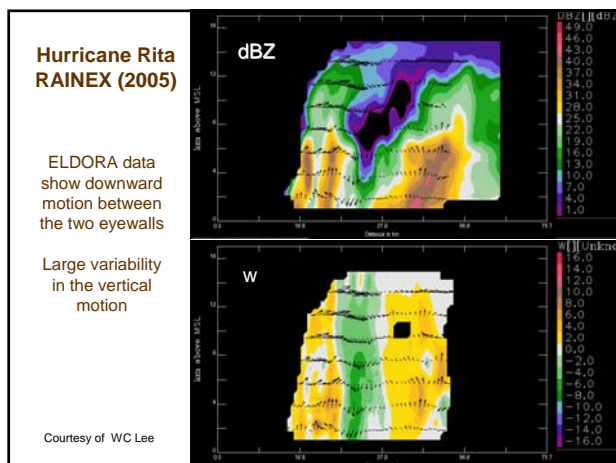
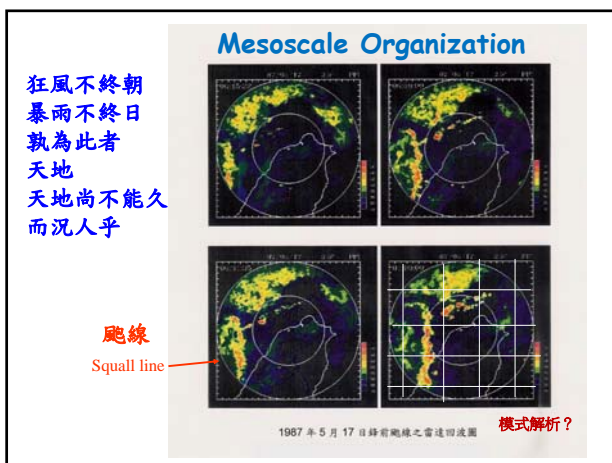
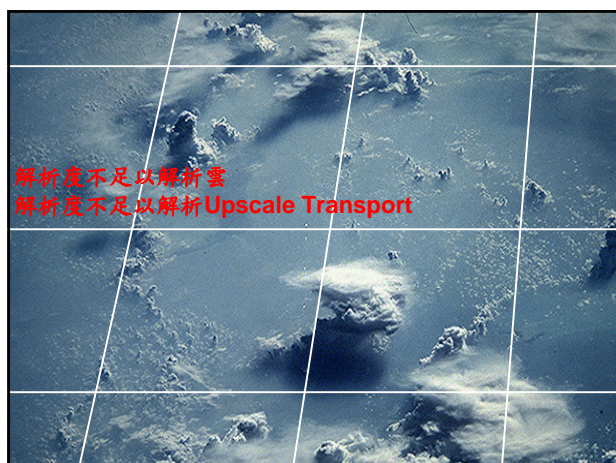


颱風潛熱與其它能量的比較

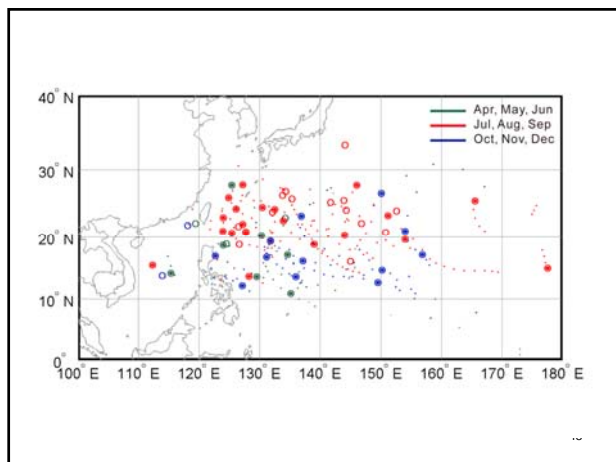
賀伯颱風的全台灣平均總雨量
為 400mm
 $400\text{ mm} = 0.4\text{ m}$
 $0.4\text{ m} * 1000\text{ kg m}^{-3} \approx 2.5 \times 10^6 \text{ J kg}^{-1}$
 $= 10^9 \text{ J m}^2$
 $10^9 \text{ J m}^2 * 3.5 \times 10^{10} \text{ m}^2$
 $= 3.5 \times 10^{19} \text{ J} \sim 10^{20} \text{ J}$

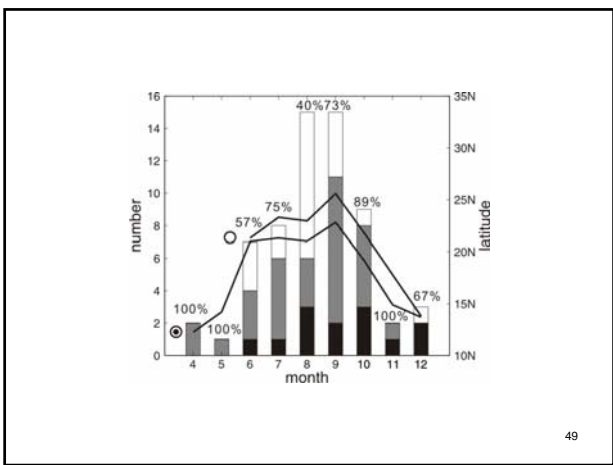
${}_0^1\text{n} + {}_{92}^{235}\text{U} \rightarrow {}_{56}^{142}\text{Ba} + {}_{36}^{91}\text{Kr} + 3 {}_0^1\text{n}$
 $1.68 \times m * 10^{13} \text{ J/mol}$
 $\Rightarrow 1.46 \times 10^6 \text{ kg U}^{235} (6 \times 10^6 \text{ mol})$

能量估計值		備註
賀伯颱風降雨總潛熱能量	10^{20} J	可使台灣整層大氣增溫 100 度
台灣一年用電量	$5 \times 10^{17} \text{ J}$	需數百年用電量才相當
全世界核子彈爆炸釋放能量	$2 \times 10^{19} \sim 2 \times 10^{20} \text{ J}$	與賀伯颱風同等級
核戰後燃燒釋放能量	$2 \times 10^{20} \text{ J}$	與賀伯颱風同等級
地球一天接受的太陽能量	$1.5 \times 10^{22} \text{ J}$	數百個賀伯颱風
Tunguska隕石撞地球（西元1908年，西伯利亞）	10^{16} J	賀伯颱風的萬分之一
火流星撞地球（恐龍滅絕？）	$4 \times 10^{23} \text{ J}$	數千個賀伯颱風

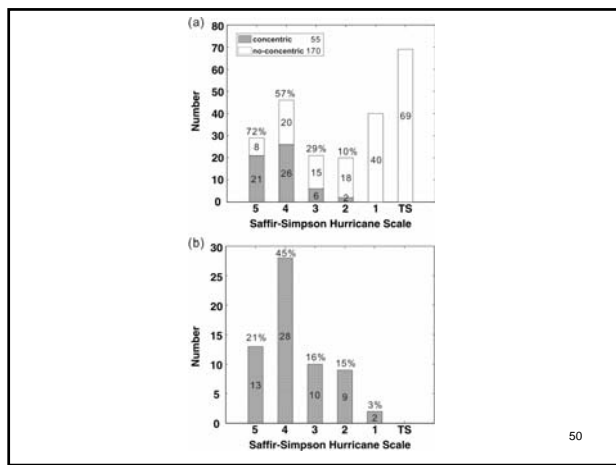


47

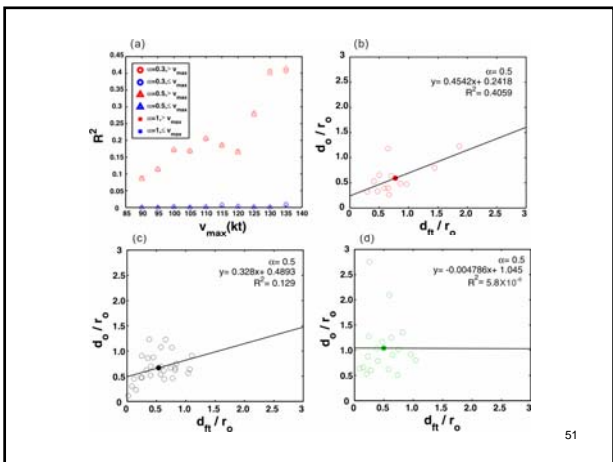




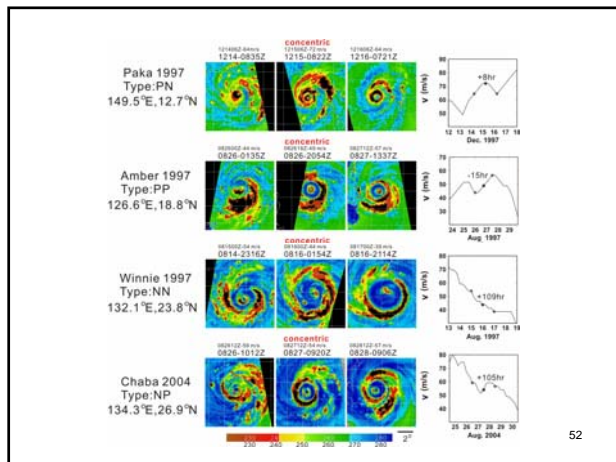
49



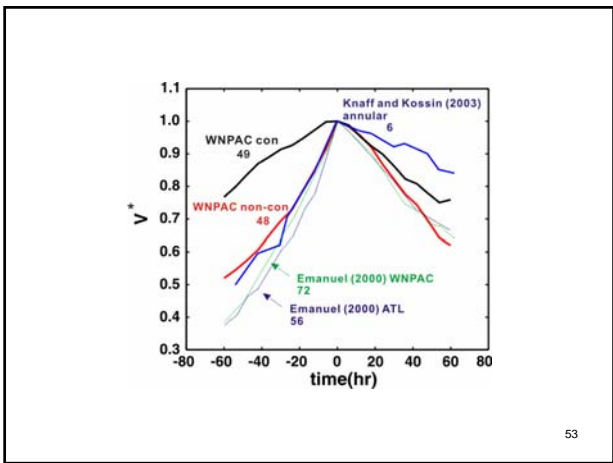
50



51



52



53

